



## Molecular Crystals and Liquid Crystals

Publication details, including instructions for authors and subscription information:

<http://www.tandfonline.com/loi/gmcl20>

### Influence of Deposition Rate on Optical Properties of RF-Magnetron Sputtered Carbon-Nickel Composite Films Deposited at Different Deposition Times

S. Mohammad Elahi<sup>a b</sup>, Vali Dalouji<sup>a</sup>, Dariush Mehrparvar<sup>a</sup> & Shahoo Valedbagi<sup>b</sup>

<sup>a</sup> Department of Physics, Razi University, Kermanshah, Iran

<sup>b</sup> Plasma Physics Research Center, Science and Research Branch, Islamic Azad University, Tehran, Iran

Published online: 16 Dec 2013.

To cite this article: S. Mohammad Elahi, Vali Dalouji, Dariush Mehrparvar & Shahoo Valedbagi (2013) Influence of Deposition Rate on Optical Properties of RF-Magnetron Sputtered Carbon-Nickel Composite Films Deposited at Different Deposition Times, *Molecular Crystals and Liquid Crystals*, 587:1, 105-112, DOI: [10.1080/15421406.2013.821586](https://doi.org/10.1080/15421406.2013.821586)

To link to this article: <http://dx.doi.org/10.1080/15421406.2013.821586>

PLEASE SCROLL DOWN FOR ARTICLE

Taylor & Francis makes every effort to ensure the accuracy of all the information (the "Content") contained in the publications on our platform. However, Taylor & Francis, our agents, and our licensors make no representations or warranties whatsoever as to the accuracy, completeness, or suitability for any purpose of the Content. Any opinions and views expressed in this publication are the opinions and views of the authors, and are not the views of or endorsed by Taylor & Francis. The accuracy of the Content should not be relied upon and should be independently verified with primary sources of information. Taylor and Francis shall not be liable for any losses, actions, claims, proceedings, demands, costs, expenses, damages, and other liabilities whatsoever or howsoever caused arising directly or indirectly in connection with, in relation to or arising out of the use of the Content.

This article may be used for research, teaching, and private study purposes. Any substantial or systematic reproduction, redistribution, reselling, loan, sub-licensing, systematic supply, or distribution in any form to anyone is expressly forbidden. Terms &



# Influence of Deposition Rate on Optical Properties of RF-Magnetron Sputtered Carbon–Nickel Composite Films Deposited at Different Deposition Times

S. MOHAMMAD ELAHI,<sup>1,2</sup> VALI DALOUJI,<sup>1,\*</sup>  
DARIUSH MEHRPARVAR,<sup>1</sup> AND SHAHOO VALEDBAGI<sup>2</sup>

<sup>1</sup>Department of Physics, Razi University, Kermanshah, Iran

<sup>2</sup>Plasma Physics Research Center, Science and Research Branch, Islamic Azad University, Tehran, Iran

*In this work, the optical properties of carbon–nickel films deposited at different deposition times from 50 to 600 sec were investigated. Reflectance measurements in wavelength range 300–1000 nm were used to compute the refractive index and optical dispersion parameters according to Wemple and DiDomenico single oscillator model (WDD). Dispersion curves of the refractive index of films show anomalous dispersion in absorption region and normal dispersion in transparent region. It is shown that dissipative rate of the electromagnetic wave at 180 sec has a maximum value. It is also shown that at 180 sec films become more disordered.*

**Keywords** Carbon–nickel; deposition rate; deposition times; RF-magnetron

## 1. Introduction

Recently, much attention has been given to amorphous carbon (a-c) films containing metals (Me = Au, Ag, Cu, Mn, etc.) due to their low cost and wide variety of properties [1–10]. Because of their interesting properties, a-c:Me have many applications as coating materials in biomedical, electronic, mechanic, and optics [11–16]. The advantage of a-c:Me films as electronic materials is that their conductivity behavior can be changed from dielectric to metallic by slight variation in their composition [10]. Also, incorporation of metal atoms may induce other interesting properties such as a way to control stress and adhesion of the films [16]. Knowledge of the optical constant such as refractive index, extinction coefficient, and dielectric constant of these films are important for designing of new materials [17,18]. Optical constants include the valuable information for technological applications [17,18]. Furthermore, the change in refractive index is important for controlling optical properties of the films because optical properties are directly related to their structural and electronic properties [19]. An element such as Ni with low or without affinity to carbon atom leads to a relatively sharp interface between the carbon matrix and the metallic phase and therefore distinct properties are produced in comparison to carbide forming elements [20,21]. Moreover, nickel–carbon composite films are studied for their interesting properties such as residual stress reduction for hard films [22], improvement of the dielectric constant

---

\*Address correspondence to Vali Dalouji, Department of Physics, Razi University, Kermanshah, Iran. E-mail: dalouji@yahoo.com

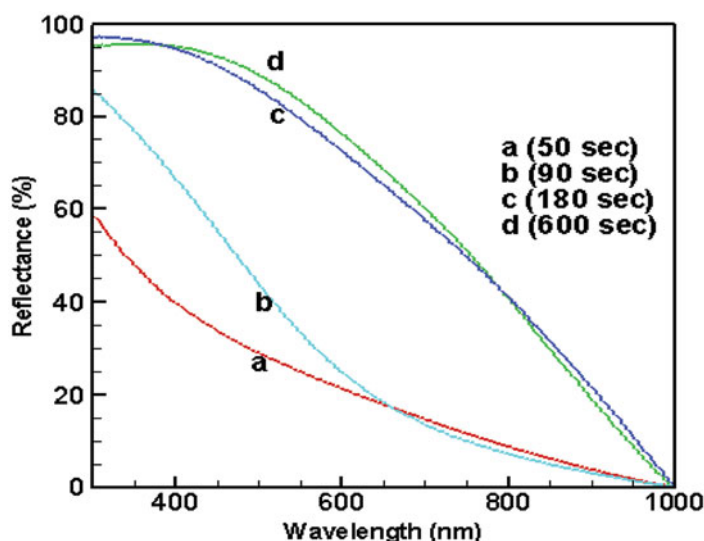


**Figure 1.** The optical reflectance spectra of the C–Ni thin films at different deposition times as a function of wavelength.

[23], or decrease of the friction coefficient [22] in conditions where constant deposition rates are synthesized. The optical properties of films are strongly affected by different deposition rates. In the present work, we investigated the effect of different deposition rates on the optical properties of amorphous C–Ni films. We used the RF-magnetron co-sputtering deposition technique for syntheses of films.

## 2. Experimental Details

Carbon–nickel composite films have been prepared by RF-magnetron co-sputtering onto quartz substrates using a multi-component target (10 cm in diameter) consisting of pure graphite (99.99%) and strips of pure nickel (approximately 2 cm<sup>2</sup>) attached to the graphite race track, which corresponds to approximately 2.5% in area. Before loading in the deposition chamber, the substrates were ultrasonically cleaned in acetone bath for 20 min and then were dried in hot air flow. The films were grown at room temperature in a deposition chamber evacuated to a base pressure  $5 \times 10^{-5}$  mbar, and then the constant Ar working pressure of  $4 \times 10^{-2}$  mbar was settled and maintained by throttle valve. Deposition was done in constant RF power regime of 400 W. We prepared films at different deposition times of 50, 90, 180, and 600 sec. The thickness of the films was measured by Tencor Alpha-step 500 profiler. The deposition rate of films at deposition times 50, 90, 180, and 600 sec are estimated by 0.84, 1.6, 1.71, and 1 nm sec<sup>-1</sup>, respectively. AFM analysis on non-contact mode was used to obtain surface morphology properties. The absorption and transmittance spectra were obtained by a double beam UV-vis spectrometer (Jasco v-630) in the range of 250–1000 nm.

## 3. Result and Discussion

Figure 1 shows the optical reflectance spectra of the C–Ni thin films with different Ni contents, respectively. As is expected, by increasing deposition time the reflectance increases.

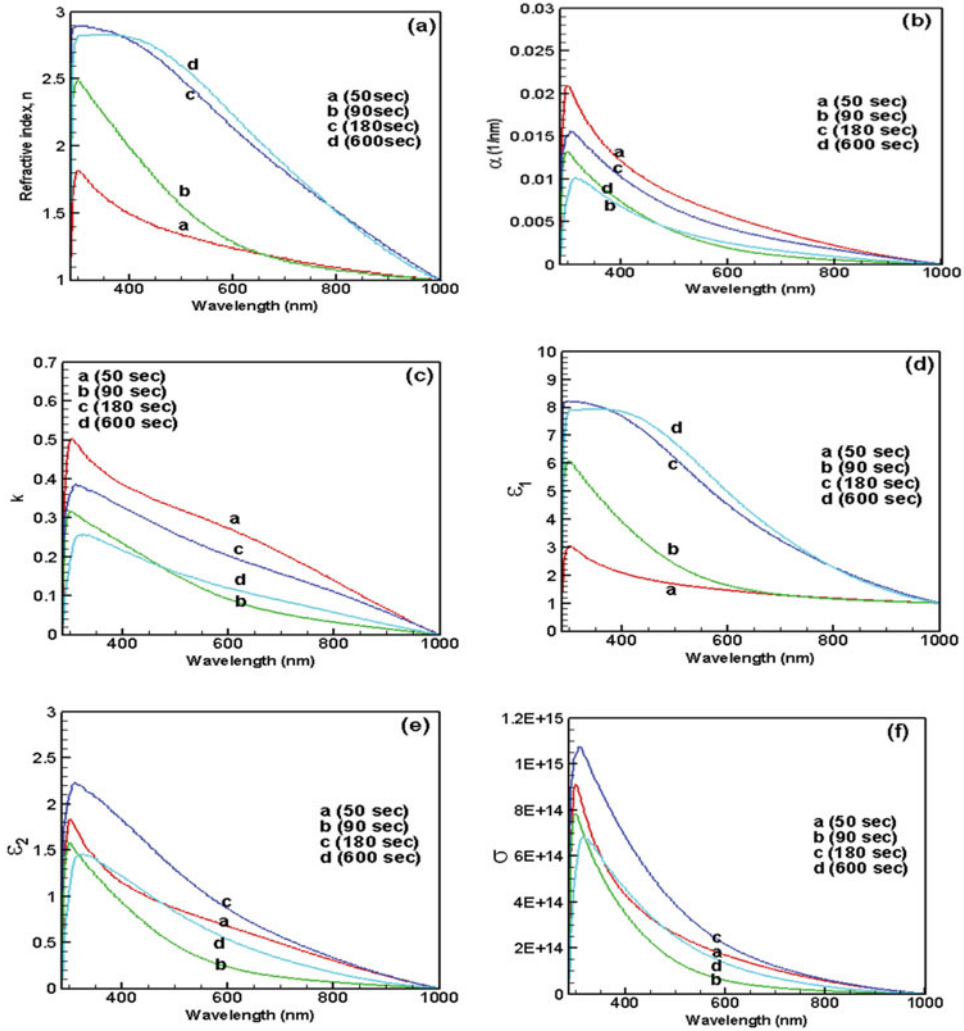


**Figure 2.** The variation of the optical parameters,  $n$ ,  $\alpha$ ,  $k$ ,  $\epsilon_1$ ,  $\epsilon_2$ , and  $\sigma$  of the C–Ni films deposited at different times as a function of wavelength.

The high reflectance in high deposition times is caused by the interaction of the light with high free electrons that are present in the metal [18]. As is shown in Fig. 1, the effect of deposition rate at 180 sec in parts of wavelength range was even greater than the effect of deposition times.

Figure 2 shows the optical parameters value at different deposition times of 50 to 600 sec as a function of wavelength. The refractive index,  $n$ , was calculated by the following equation [24]:

$$n = \frac{(1 + R^{\frac{1}{2}})}{(1 - R^{\frac{1}{2}})} \quad (1)$$

As shown in Fig. 2(a), the refractive index decreases with increasing the wavelength for the investigated films. However, the refractive index attain a peak at a wavelength about  $\lambda = 300$  nm in absorption region. The refractive index shows an anomalous dispersion at the lower wavelengths and a normal dispersion at the higher wavelengths. By increasing of deposition time up to 180 sec, the refractive index increases; however, above 180 sec it increases very slowly (for all of wavelength range). It is due to decreasing of deposition rate at deposited films at 600 sec. Figures 2(b) and (c) show the absorption edge and extinction coefficient films deposited at 50–600 sec as a function of wavelength. The film deposited at 50 sec has very low thickness with respect to other films; therefore, it has a high absorption edge and hence a high extinction coefficient [25,26]. Due to increasing of deposition rate and hence increasing of localized states (Fig. 2(c)) in to band gap, the absorption edge increases; however, because of decreasing deposition rate at 600 sec, the absorption edge and the extinction coefficient decreases [17,25,26]. Figures 2(d) and (e) show the real and imaginary parts of the complex dielectric function of the films deposited at 50–600 sec as a function of wavelength. The real parts of the dielectric constant of the films are higher than of imaginary part. The real part of the dielectric constant relates to dispersion, whereas the dissipative rate of the electromagnetic wave in the dielectric medium is provided by imaginary part. As shown in Fig. 2(e), the dissipative rate of the electromagnetic wave at 180 sec is higher than other films. Figure 2(f) shows the optical conductivity of films deposited at 50–600 sec as a function of wavelength. The optical conductivity of films are given by  $\sigma = anc/4\pi$ , where  $\alpha$  is the absorption coefficient,  $n$  is the refractive index, and  $c$  is the velocity of light [27]. The RMS roughness of the films deposited at 50, 90, 180, and 600 sec are 3.5, 4.9, 5, and 4 nm, respectively. By increasing the deposition time from 50 to 90 sec due to increasing RMS roughness, and hence decreasing absorption edge, the optical conductivity decreases. However, by increasing deposition time up to 180 sec because of increasing deposition rate, hence increasing density of localized states within gap, the optical conductivity increases, and at 600 sec, due to decreasing localized state, the optical conductivity decreases [17,28].

Figures 3(a) and (b) show the variation of  $(\alpha h\nu)^2$  and  $(\alpha h\nu)^{1/2}$  versus  $h\nu$  for films as a function of deposition time, respectively. The absorption coefficient of semiconductors is known to change rapidly for photon energies close to their band gap and can be divided into two regions according to the values of absorption coefficient [29–31]. For the first region for the higher values of the absorption coefficient, the optical absorption edge was analyzed by the Tauc power law for optical transition using the relation  $(\alpha h\nu)^n = A(h\nu - E_g)$  [29–31], where  $A$  is constant,  $E_g$  is the optical energy gap, and  $n$  determines the type of the optical transition ( $n = 2$  for allowed direct,  $n = 1/2$  for allowed indirect,  $n = 1/3$  for forbidden indirect, and  $n = 2/3$  for forbidden direct optical transitions).

We found that direct band gap for the films deposited at 50, 90, 180, and 600 sec are 4.34, 4.40, 4.39, and 4.40 eV, respectively. We also found that indirect band gap for the films deposited at 50, 90, 180, and 600 sec are 1.46, 1.94, 1.87, and 1.94 eV, respectively. For the second region (Fig. 3(c)), the absorption at the lower photon energy usually follows the Urbach's rule using the relation  $\alpha(\nu) = \alpha_0 \exp(h\nu/E_U)$  [29–31], where  $\nu$  is the frequency of the radiation,  $\alpha_0$  is a constant,  $h$  is the Plank's constant, and  $E_U$  is Urbach's energy that is interpreted as the width of the tails of localized states in band gap and in general represents the degree of disorder in the amorphous semiconductors. The absorption in this region is due to transitions between extended states in one band and localized states in the exponential tail of the other band. We found that Urbach's energy  $E_U$  for films deposited at 50, 90, 180, and 600 sec are 1.58, 1.75, 1.88, and 1.53 eV, respectively. This data show that by increasing deposition time up to 180 sec, the width of the tail of localized states in

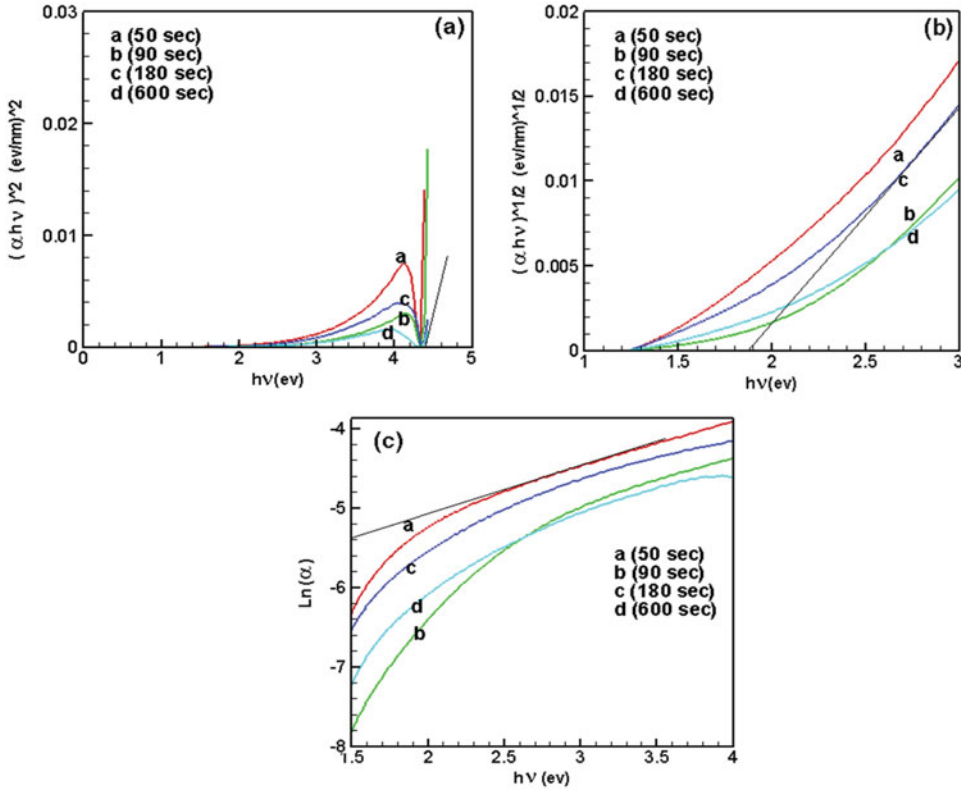


**Figure 3.** The plots of (a)  $(\alpha h\nu)^2$ , (b)  $(\alpha h\nu)^{1/2}$ , and (c)  $\ln \alpha$  for the C–Ni films deposited at different times as a function of incident photon energy.

the band gap region increases and then above 180 sec it decreases. It is due to increasing of Ni content with respect to C content up to 180 sec, but for films deposited at 600 sec the effect of the increase of the metal content is all the more marked, as the reactivity of the metal toward carbon is limited, which could indicate the introduction of defects in the band gap due to the metal implantation. However, this was not observable at the scale probed by XRD.

In the normal dispersion region, the refractive index dispersion can be analyzed by the single-oscillator model proposed by the Wemple–DiDomenico (WDD) [32–35]:

$$n^2 = 1 + \frac{E_d E_0}{E_0^2 - (h\nu)^2}, \quad (2)$$

where  $n$  is the refractive index,  $h$  is Planck's constant,  $\nu$  is the frequency,  $h\nu$  is the photon energy,  $E_0$  is the average excitation energy for electronic transitions, and  $E_d$  is the dispersion energy, which is a measure of the strength of inter-band optical transitions. Figure 4(a) shows the plots of  $1/(n^2-1)$  versus  $(h\nu)^2$  for deposited films at different times from 50 to 600 sec. By fitting data to a straight line, from the intercept  $E_0/E_d$  and slope  $1/E_0 E_d$ ,  $E_0$  and  $E_d$  can be determined. Furthermore, as was proposed by Tanaka, the first approximate value of the optical band gap  $E_g^{\text{opt}}$  is also derived from the WDD model and is given by:  $E_g^{\text{opt}} \approx E_0/2$ . Obviously, the value obtained is almost in agreement with that obtained from

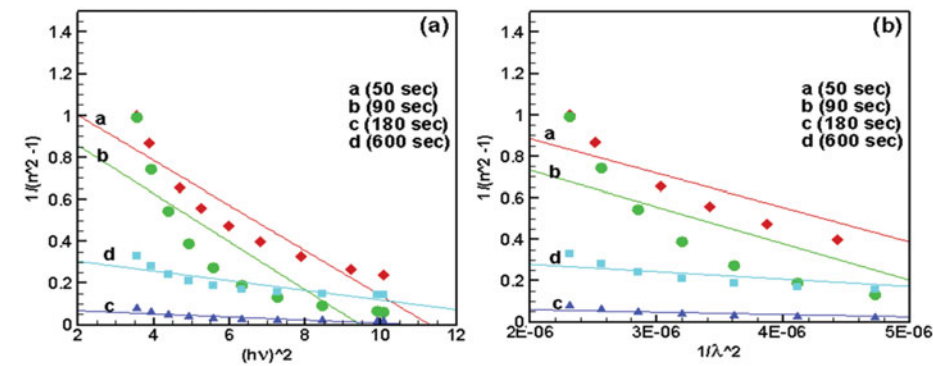


**Figure 4.** (a) and (b): The plots of  $1/(n^2-1)$  versus  $(h\nu)^2$  and  $\lambda^{-2}$  for the C-Ni films deposited at different times, respectively.

the Tauc extrapolation model. The static refractive index  $n_0$  for the films is calculated by Eq. (2) and the incident photon energy  $E$  equals to zero:

$$n_0 = (1 + E_d/E_0)^{1/2} \tag{3}$$

Average oscillator wavelength  $\lambda_0$  and oscillator length strength  $s_0$  for the films at different times can be determined using the following relationship:

$$\left(\frac{n_0^2 - 1}{n^2 - 1}\right) = 1 - \left(\frac{\lambda_0}{\lambda}\right)^2, \tag{4}$$

where  $\lambda_0$  values were calculated from the linear parts of the plots of  $n^2 - 1$  versus  $\lambda^{-2}$  (Fig. 4(b)). It is shown that Eq. (4) can also be written as

$$n^2 - 1 = \frac{s_0}{1 - (\frac{\lambda_0}{\lambda})^2} \tag{5}$$

where  $s_0 = (n_0^2 - 1) / \lambda_0^2$ . The optical moments  $M_{-1}$  and  $M_{-3}$  of the optical spectra for the films can be written as:

$$E_0 = \frac{M_{-1}}{M_{-3}}, \quad E_d^2 = \frac{M_{-1}^3}{M_{-3}} \tag{6}$$

These results are listed in Table 1.

**Table 1.** Optical parameters of C-Ni composite films

Deposition time (sec)	$E_{\text{Urbach}}$ (eV)	$E_g^{\text{opt}}$ (eV)	$E_g^{\text{opt}}$ (WDD)	$E_0$ (eV)	$E_d$ (eV)	$\lambda_0$ (nm)	$n_0$	$M_{-1}$	$M_{-3}$ (eV) <sup>-2</sup>	$S_0$ (m <sup>-2</sup> )
50	1.58	1.46	1.52	3.04	3.04	413	1.44	1	1	$5.78 \times 10^{12}$
90	1.75	1.95	1.36	2.72	3.23	457	1.47	1.18	0.16	$5.55 \times 10^{12}$
180	1.88	1.87	1.41	2.82	40.4	717	3.91	7.24	0.23	$27.77 \times 10^{12}$
600	1.53	1.94	1.58	3.16	10.56	245	2.04	3.33	0.33	$52.63 \times 10^{12}$



#### 4. Conclusions

The optical properties of C–Ni films deposited at different deposition times from 50 to 600 sec were investigated. It has been observed that the deposition rate of the deposited has an important influence on the optical properties of the C–Ni films. We noticed that refractive index, absorption coefficient, extinction coefficient, the real and imaginary parts of the dielectric constant, and the optical conductivity increase by increasing of deposition rate. The optical dispersion parameters were also calculated. The dispersion curves of the refractive index of films have both anomalous dispersion in the absorption region and normal dispersion in the transparent region. It is shown that the dissipative rate of the electromagnetic wave at 180 sec has a maximum value. The films deposited at 180 sec have a maximum disordered value ( $E_U = 1.88$  eV).

#### References

- [1] Endrino, J. L., Escobar Galindo, R., Zhang, H. S., Allen, M., Gago, R., Espinosa, A., & Anders, A. (2008). *Surf. Coat. Technol.*, 202, 3675.
- [2] Hauert, R. (2003). *Diamond Relat. Mater.*, 12, 583.
- [3] Narayan, R. J. (2005). *Diamond Relat. Mater.*, 14, 1319.
- [4] Chang, Y. Y., Wang, D. Y., & Wu, W. (2002). *Thin Solid Films*, 420–421, 241.
- [5] Baba, K., & Hatada, R. (2002). *Surf. Coat. Technol.*, 158–159, 272.
- [6] Wang, R., Mercer, C., Evans, A. G., Cooper, C. V., & Yoon, H. K. (2002). *Diamond Relat. Mater.*, 11, 1797.
- [7] Nilsson, D., Svahn, F., Wiklund, U., & Hogmark, S. (2003). *Wear*, 252, 1084.
- [8] Okpalugo, T. I. T., Maguire, P. D., Ogwu, A. A., & McLaughlin, J. A. D. (2004). *Diamond Relat. Mater.*, 13, 1549.
- [9] Zhang, P., Tay, B. K., Yu, G. O., Lau, S. P., & Fu, Y. Q. (2004). *Diamond Relat. Mater.*, 13, 459.
- [10] Ghodselahi, T., Vesaghi, M. A., Shafiekhani, A., Ahmadi, M., Panahandeh, M., & Heidari Saani, M. (2010). *Physica B*, 405, 3949.
- [11] Zong, C. J., Luo, J., Fang, B., Wanjala, B. N., & Njoki, P. N. (2010). *Nanotechnology*, 21, 1.
- [12] Korotcenkov, G., Han, S. D., & Stetter, J. R. (2009). *Chem. Rev.*, 10, 1402.
- [13] Kambhampati, D. K., & Knoll, W. (1999). *Curr. Opin. Colloid Interface Sci.*, 4, 273.
- [14] Tanabe, K. (2007). *Mater. Lett.*, 61, 4573.
- [15] Chen, Y., Munechika, K., & Ginger, D. S. (2007). *Nano Lett.*, 7, 690.
- [16] Khlebtsov, N. G., Dykman, L. A., & Quant, J. (2010). *Spectrosc. Radiat. Transfer*, 111, 1.
- [17] Wasa, K., Kitabatake, M., & Adachi, H. (2003 and 2004). *Thin Film Materials Technology: Sputtering of Compound Material*, William Andrew: Norwich, NY.
- [18] Fox, M. (2001). *Optical Properties of Solids*, Oxford University Press: New York.
- [19] Robertson, J. (2002). *Mater. Sci. Eng. R.*, 37, 129.
- [20] Endrino, J. L., Horwat, D., Gago, R., Andersson, J., Liu, Y. S., Guo, J., & Anders, A. (2009). *Solid State Sci.*, 11, 1742.
- [21] Ghodselahi, T., Vesaghi, M. A., Shafiekhani, A., Baradaran, A., Karimi, A., & Mobini, Z. (2008). *Surf. Coat. Technol.*, 202, 2731.
- [22] KuKielka, S., Gulbinski, W., Pauleau, Y., Dub, S. N., & Grob, J. J. (2006). *Surf. Coat. Technol.*, 200, 6258.
- [23] Sbai-Benchikh, N., Zeinert, A., Caillierez, H., & Donnet, C. (2009). *Diamond Relat. Mater.*, 18, 1085.
- [24] Egharevba, G. O., Eleruja, M. A., Osasona, O., Akinwunmi, O. O., Olofinjana, B., Jaynes, C., & Ajayi, E. O. B. (2012). *J. Mater. Sci. Res.*, 1, 130.
- [25] Montiel-Gonzalez, Z., Rodil, S. E., Muhl, S., Mendoza-Galvan, A., & Rodriguez-Fernandez, L., (2011). *Thin Solid Films*, 519, 5924.

- [26] Mott, N. F., & Davis Mott, E. A. (1979). *Electronic Processes in Non-Crystalline Materials*, Clarendon Press: Oxford.
- [27] Abbas, M. M., Shehab, A. Ab-M., Al-Samuraee, A.-K., & Hassan, N.-A. (2011). *Energy Procedia*, 6, 241.
- [28] Endrino, J. L., Horwat, D., Gago, R., Andersson, J., Liu, Y. S., Guo, J., & Anders, A. (2009). *Solid State Sci.*, 11, 1742.
- [29] Sakr, G. B., Yahia, I. S., Fadel, M., Fouad, S. S., & Romcevic, N. (2010). *J. Alloys. Compd.*, 507, 557.
- [30] Majeed Khan, M. A., Kumar, S., Ahamed, M., Alrokayan, S. A., Alsalhi, M. S., Alhoshan, M., & Aldwayyan, A. S. (2011). *Appl. Surf. Sci.*, 257, 10607.
- [31] Habibi, M. H., & Talebian, N. (2005). *Acta Chim. Slov.*, 52, 53.
- [32] Badran, H. A. (2012). *Am. J. Appl. Sci.*, 9(2), 250.
- [33] Tigau, N., Condurche-Bota, S., & Sovean, R. (2010). *J. Sci. Arts*, 2, 361.
- [34] Gholami, M. (2012). *J. Basic Appl. Res.*, 2, 3563.
- [35] Shaaban, E. R., Yahia, I. S., & EL-Metwally, E. G. (2012). *Acta. Phys. Polo. A*, 121, 628.